Tuijin Jishu/Journal of Propulsion Technology
ISSN: 1001-4055
Vol. 47 No. 02 (2026)

Evaluating the Dynamics of Land Use and Land Cover Changes in Relation to the Land Surface Temperature of Hyderabad City

Pardeep Kumar[1,2*], Pratyush Verma[1], Saumitra Mukherjee[1], Bhawna Yadav[1], Bir Abhimanyu Kumar[3]

[1]School of Enviornmental Sciences, Jawaharlal Nehru University, New Delhi-110067, India.
[2]National Accreditation Board of Education and Training, Quality Council of India, New Delhi-110067, India.
[3]Department of Elementary Education, NIE, NCERT, New Delhi-110016
[*]Corresponding Author-

Abstract:- Land Surface Temperature (LST) is a critical indicator of urban thermal comfort and heat stress. This study investigates the relationship between land use/land cover (LULC) changes and LST dynamics in Hyderabad City, India, over a 30-year period (1989–2019) using decadal Landsat imagery. The satellite data were pre-processed through radiometric and atmospheric correction, and classified into four LULC classes-built-up, barren land, vegetation, and water bodies-using the Support Vector Machine (SVM) algorithm. LST was retrieved using mono-window algorithms, while the Contribution Index (CI) was employed to quantify the thermal impact of each LULC class. Results reveal a significant expansion of built-up areas from 35.8% to 56.5%, alongside a decline in barren land (42.7% to 33.4%), vegetation (19.4% to 8.2%), and water bodies (2.1% to 2.0%). The warming effect of barren land decreased (CI from 0.58 to 0.22), while the cooling influence of vegetation (CI from -0.42 to -0.06) and water bodies (CI from -0.14 to -0.10) also weakened over time. Declining values of the Normalized Difference Vegetation Index (NDVI) and Normalized Difference Water Index (NDWI) indicate reductions in vegetation health and water extent. Simultaneously, rising Normalized Difference Built-up Index (NDBI) and Normalized Difference Bareness Index (NDBaI) reflect increasing urbanization and land conversion. These findings highlight the shifting surface energy balance driven by LULC changes and provide critical insights for sustainable urban planning and climate adaptation strategies.

Keywords*: Urban Heat Island, Contribution Index, Remote Sensing, Hyderabad City, Support Vector Machine.*

1. Introduction

Climate change is manifesting in various ways across the globe, with one of the most notable being the increasing frequency, intensity, and duration of heatwave events. These extreme temperature episodes are contributing to heightened thermal discomfort, particularly in urban areas. In recent years, numerous scientific investigations have focused on characterizing the spatial and temporal patterns of temperature variability from local to global scales (Khan and Chatterjee, 2019). Urban climate change is driven by both natural processes and anthropogenic activities that alter the Earth's surface and atmospheric properties (Henderson and Gornitz, 1984).

Urbanization has intensified rapidly over the past few decades. Urban areas, which accounted for approximately 30% of the global population in the 1950s, have grown to encompass 55% by 2018 and are projected to reach 68% by 2050 (United Nations, 2014; 2018). Although the global population has increased sixfold over the last two centuries, the urban population has expanded nearly 128 times (Schell et al., 1993). This transformation has brought both opportunities and challenges-while fostering economic and social development, urbanization has also exerted intense pressure on ecosystems and natural resources.

The adverse effects of unplanned urban growth include overcrowding, degradation of living conditions, loss of permeable surfaces and vegetation, altered surface albedo, water and air pollution, and strain on water resources (Ohwo and Abotutu, 2015; Hahs et al., 2009; Zhao et al., 2006; Cui and Shi, 2012). In particular, changes in LULC profoundly influence natural cycles, habitat continuity, and local climate by modifying surface characteristics (Seto et al., 2011; Radeloff et al., 2010; Jago-on et al., 2009; Yuan, 2008).

Recent research increasingly emphasizes the connection between LULC change and LST, a key parameter in assessing urban heat dynamics. For instance, Zhao et al. (2024) demonstrated that satellite-derived indices are effective in capturing how LULC transitions affect LST in urban areas. Rees et al. (2024) found similar links in Kharkiv, Ukraine, while Gemeda et al. (2024) documented region-specific effects in Ethiopian cities. These studies underscore the utility of remote sensing in monitoring urban thermal environments.

Urbanization leads to significant modifications in the built environment and surface materials. Impervious surfaces, such as asphalt and concrete, have higher heat retention and lower emissivity compared to natural surfaces. Additionally, anthropogenic heat emissions and altered airflow due to dense structures exacerbate heat accumulation (Oke, 1987). These changes contribute to the Urban Heat Island (UHI) effect-elevated temperatures in urban cores compared to surrounding rural or peri-urban areas (Doan and Kusaka, 2015). UHI is most pronounced during nighttime and minimum temperature periods (Bahl and Padmanabhamurty, 1979; Gangadharan et al., 1999).

The UHI phenomenon has been studied globally across various climatic zones (Arnfield, 2003; Parker, 2010), and is fundamentally influenced by urban form and LULC patterns (Oke, 1995; Bridgman et al., 1995). In India, Guha and Govil (2025) explored the stability of the LULC–LST relationship in Hyderabad, emphasizing remote sensing's value in such assessments. Gogoi and Vinoj (2025) found LULC change to be a principal driver of regional air temperature trends in India.

Contributors to UHI include reduced vegetation and surface reflectivity, increased thermal conductivity of urban materials, lower evapotranspiration, and altered airflows caused by urban morphology (Kim and Baik, 2005; Chen et al., 2014). Continued urban sprawl also poses a threat to biodiversity by encroaching upon protected ecological areas (Helmers, 2010). However, urban vegetation and surface reflectivity remain two manageable levers for mitigating UHI effects (Akbari, 2009).

Both ground-based and satellite-based approaches are employed to assess urban climates. While traditional weather stations provide point-based air temperature data (Eludoyin et al., 2013; Vancutsem et al., 2010), satellite remote sensing enables comprehensive LST monitoring across spatial and temporal scales (Weng, 2009; Sobrino et al., 2012; Qiao et al., 2013). Spectral indices such as the NDVI, NDWI, NDBI, and NDBaI are particularly useful for quantifying LULC features and their thermal implications (Estoque et al., 2017; Bokaiea et al., 2016; Omran, 2012; Kawashima, 1994).

Despite extensive research, there remains a need for multi-decadal, location-specific analysis to understand the interplay between urbanization, LULC changes, and thermal conditions. Hyderabad, a major urban hub in southern India, provides an ideal case to explore these dynamics due to its rapid urban growth and climatic vulnerability.

2. Objectives

This study addresses a critical gap by providing a comprehensive, multi-temporal analysis of LULC and LST dynamics in Hyderabad from 1989 to 2019. The objectives are to (1) map decadal LULC changes using SVM classification; (2) retrieve LST via mono-window algorithm and (3) apply a CI to quantify the influence of each LULC class on urban thermal patterns. These insights aim to inform sustainable urban planning and climate adaptation strategies for Hyderabad.

3. Study Area

Hyderabad is the capital and largest city of Telangana, located in southern India. The study area includes the region surrounding Hyderabad, bounded between latitudes 17° 16′ 56″ to 17° 33′ 40″ N and longitudes 78° 14′

38″ to 78° 38′ 28″ E, covering approximately 686 square kilometers (Figure 1). The city's terrain is predominantly hilly, interspersed with several artificial lakes, and it lies along the banks of the Musi River-a tributary of the Krishna River. Hyderabad, with a population of 6.9 million people (INDIA, 2011), ranks as the fourth-most populous city in the country. It rests on sloping terrain composed of pink and grey granite, with an average elevation of 542 meters above sea level (Ramachandraia, 2013). Prominent artificial lakes in the city include Hussain Sagar, Osman Sagar, and Himayat Sagar. According to the Telangana Socio-Economic Outlook 2023 (https://des.telangana.gov.in/publications/Telangana-Socio-Economic-Outlook-2023.pdf) and projections by the Census of India, the population of Greater Hyderabad has risen substantially over the past decade, reaching an estimated 10.5 million in 2023 (https://www.macrotrends.net/global-metrics/cities/21275/hyderabad/population). This growth reflects a significant demographic shift from the 2011 Census figure of 6.8 million. The rapid population increase has been paralleled by extensive municipal expansion, with the Greater Hyderabad Municipal Corporation (GHMC) incorporating adjacent municipalities and peri-urban zones. This administrative and spatial growth has significantly intensified land use transformation, converting vegetated and barren land into built-up areas to accommodate residential, commercial, and infrastructural demands (https://worldpopulationreview.com/cities/pakistan/hyderabad?).

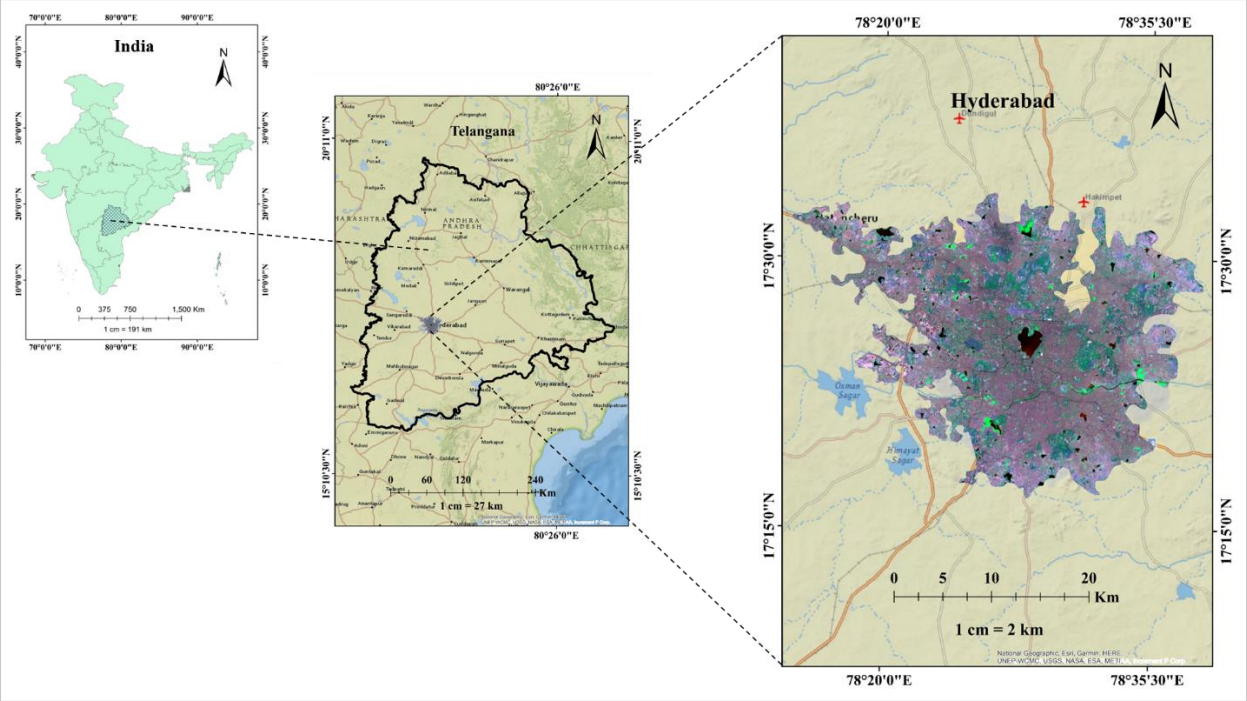

Figure 1. Study area map of Hyderabad city

Hyderabad features a hot semi-arid climate with distinct dry and wet seasons, governed primarily by the southwest monsoon. Recent climate assessments based on long-term meteorological records (https://weatherspark.com/y/109450/Average-Weather-in-Hyderabad-Telangana-India-Year-Round) indicate that the annual average temperature hovers around 27°C, with monthly means ranging from 21°C in December to 33°C in May. The hottest month is May, which records average daily highs of 38°C to 39°C (101°F) and lows around 27°C (81°F), while the coolest month is December, with average lows of 16°C (61°F) and highs of 28°C (83°F). Although historic extremes include a high of 45.4°C on June 2, 1966, and a low of 6.1°C on January 8, 1946, recent observations suggest that temperatures rarely fall below 13°C (55°F) or exceed 42°C (107°F).

The monsoon season spans from June to September, with July and August being the rainiest months, receiving average monthly rainfall of up to 6.1 inches (155 mm). The wettest single-day event on record delivered 241.5 mm of rain on August 24, 2000 (IMD). Cloud cover during the monsoon months typically exceeds 85–90%, contributing to elevated humidity levels of over 75%, while January to March remain the clearest and driest

months, with cloud cover below 25% and humidity levels as low as 25–30% (https://mausam.imd.gov.in/hyderabad/).

Sunshine duration shows significant seasonal variation, with February typically experiencing the highest daily sunlight exposure. The city receives approximately 2,700 hours of sunshine annually. Wind speeds are highest during July (up to 13.2 mph), coinciding with peak monsoonal activity, while October is the calmest period. These dynamic climatological patterns, coupled with Hyderabad's rapid urban growth, have direct implications for LST, urban heat stress, and sustainable land-use planning (https://mausam.imd.gov.in/hyderabad/)

4. Methods

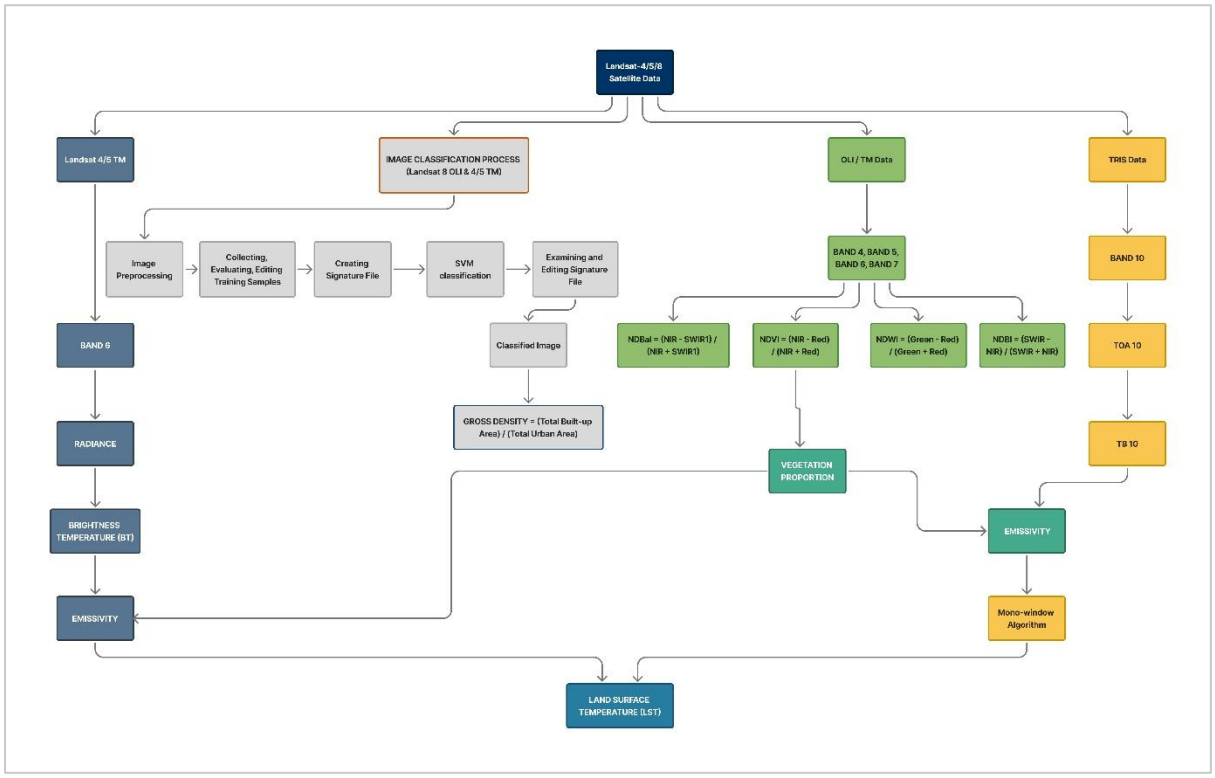

Figure 2. Integrated workflow of Landsat 4/5/8 data for deriving LST and SVM classification

Table 1. Satellite data for the study area

Satellite	Date	Time	Path/Row	Cloud Cover
Landsat 8 OLI	25-02-2019	05:09	144/048	0%
Landsat 4–5 TM	13-02-2009	04:55	144/048	0%
Landsat 4–5 TM	18-02-1999	04:48	144/048	0%
Landsat 4–5 TM	22-02-1989	04:49	144/048	0%

Landsat 8 provides 11 multispectral bands, while Landsat 4–5 offers 7 bands categorized into visible, near-infrared (NIR), shortwave infrared (SWIR), and thermal infrared bands. Landsat 4–5 satellites are equipped with the Multispectral Scanner (MSS) and Thematic Mapper (TM) sensors, whereas Landsat 8 carries the Operational Land Imager (OLI) and Thermal Infrared Sensor (TIRS) (Table 1). Satellite imagery for the years 1989, 1999, 2009, and 2019 was obtained from the United States Geological Survey (USGS) EarthExplorer platform (https://earthexplorer.usgs.gov/). These bands were stacked using ERDAS IMAGINE software, and LST was derived using ArcGIS. The years 1989, 1999, 2009, and 2019 were selected to represent decadal intervals, allowing for a systematic temporal analysis of LULC dynamics and corresponding changes in LST over a 30-year period (Figure 2). This decadal approach provides a balanced and consistent timeline to observe long-term urbanization trends, thermal anomalies, and the progression of land transformation in Hyderabad

4.1 SVM Classification

SVM is a supervised machine learning technique widely used for classification and regression. Known for its high accuracy in handling high-dimensional datasets, SVM is particularly suitable for remote sensing image classification. It functions as a binary classifier by constructing an optimal hyperplane in a high-dimensional feature space, and can employ both linear and non-linear kernels (Khan and Syed, 2015).

SVM classification was carried out in ArcGIS. First, signature files (training samples polygons) uniformly in each class (approx. 15-20% of area) were generated based on visual interpretation of land features using google earth pro and ArcMap base map. These files were used to train the SVM classifier (source: ArcGIS SVM Classifier) and to evaluate classification accuracy using the ArcGIS Accuracy Assessment tool. The classification was performed using the "Classify Raster" tool, and accuracy was assessed using 55 reference polygons through the "Compute Confusion Matrix" conducted using the ArcMap "Classify Raster" tool, across four LULC classes (built-up, vegetation, barren land, and water bodies) for each temporal dataset (1989, 1999, 2009, and 2019) (Figure 2). While the number of training samples may appear limited, ArcMap's SVM classifier is well-suited for high-dimensional data classification using small, high-quality training sets, particularly when class boundaries are spectrally distinct.

4.2 Indices Used

Several remote sensing indices were calculated to analyze land cover features and urban thermal characteristics:

1. **NDVI** = (NIR - Red) / (NIR + Red) (Equation 1)
2. **NDWI** = (Green - Red) / (Green + Red) (Equation 2)
3. **NDBI** = (SWIR – NIR) / (SWIR + NIR) (Equation 3)
4. **NDBaI** = (NIR – SWIR1) / (NIR + SWIR1) (Equation 4)

Wavelength references:

- Red: 0.560 µm
- Green: 0.655 µm
- NIR: 0.865 µm
- SWIR: 1.610 µm
- SWIR1: 2.200 µm

4.3 LST Estimation Algorithms

The Mono-Window Algorithm algorithms was used to estimate LST. The MWA was chosen for its compatibility with Landsat 8's spectral configuration and ease of operational use. It was developed by Wang et al. (2015), and calculates LST from Landsat TM data using the following formula:

Ts = [a10(1−C10−D10) + (b10 (1−C10−D10) + C10 + D10) T10−D10Ta] / C10 C10 = τ10ε10 D10 = (1−τ10) [1+(1−ε10) τ10 (Equation 5)

Where:

- **a_{10} = –62.7182**, **b_{10} = 0.4339** (model constants for 0–50°C range)
- **T_{10}** = thermal band brightness temperature
- **ε_{10}** = emissivity derived from NDVI
- **τ_{10}** = atmospheric transmittance
- **Ta** = near-surface air temperature (from meteorological stations)
- **$C_{10} = \tau_{10}\varepsilon_{10}$**
- **$D_{10} = (1 - \tau_{10})[1 + (1 - \varepsilon_{10})\tau_{10}]$**

This method was applied to Landsat TM data with local meteorological data for air temperature input.

4.4 Gross Density

Gross density is a key metric for assessing the intensity of urban land development. It is defined as the ratio of the total built-up area to the total area of the urban region:

Gross Density = Total Built-up Area / Total Area of the Urban Area (Equation 6)

A higher gross density indicates more compact urban development, characterized by a greater concentration of built structures within a given land area. Conversely, lower gross density values reflect more dispersed or low-intensity development, where built-up areas are spread over larger extents of land (Shaban et al., 2020; Sridhar and Monkkonen, 2024).

4.5 Contribution Index

CI was calculated to quantify the relative impact of each LULC class on the overall LST change.

The CI was calculated as: CI = (Area of LULC class × ΔLST) / Σ (Area × ΔLST) (Equation 7)

A higher CI implies greater contribution (Abdulmana et al., 2021).

5. Results

5.1 SVM Classification

SVM classification categorized the Hyderabad region into four LULC classes-water bodies, vegetation, barren land, and built-up areas-for the years 1989, 1999, 2009, and 2019 (Figure 3). The method achieved accuracy levels between 85% and 93% and Kappa coefficients ranging from 0.89 to 0.94 (Table 2), consistent with the performance of SVM in remote sensing classification as highlighted by Melgani and Bruzzone (2004) and Khan and Syed (2015).

Table 2. A summary of SVM classification accuracy

Year	Overall Accuracy	Kappa Coefficient
1989	88.3%	0.84
1999	89.5%	0.86
2009	90.1%	0.87
2019	92.4%	0.91

In 2019, the share of built-up areas increased to 56.49%, overtaking other land classes. Simultaneously, barren land decreased to 33.42%, while vegetation slightly increased to 8.20%. Water bodies were further reduced to 1.89%, reflecting the urban encroachment on aquatic ecosystems, a trend corroborated by other Indian metropolitan studies (Nagendra et al., 2013).

For 2009, SVM classification showed built-up areas at 49.10%, and vegetation slightly increased to 14.42%, while barren land and water bodies declined to 34.46% and 2.02%, respectively. The increasing urban footprint during this period corresponds with Hyderabad's real estate boom and population growth.

In 1999, barren land remained dominant at 44.40%, followed by built-up areas (39.55%). Vegetation dropped to 13.60%, and water bodies slightly rose to 2.45%.

In 1989, barren land accounted for 42.73%, built-up areas 35.81%, vegetation 19.39%, and water bodies 2.07%, reflecting a more ecologically diverse landscape prior to rapid urbanization.

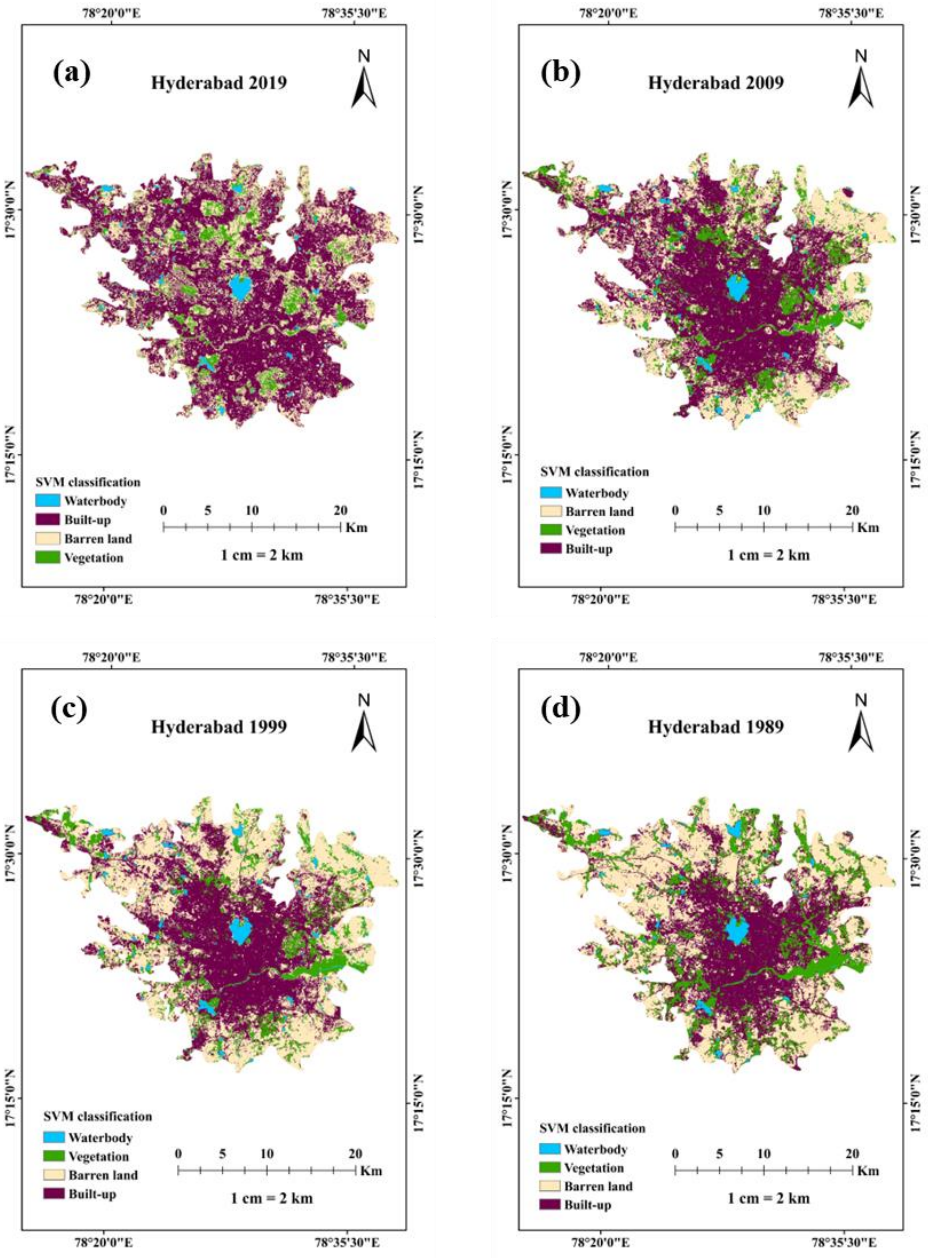

Figure 3. SVM Classification of Hyderabad Region for the Years (a) 2019, (b) 2009, (c) 1999 and (d) 1989

5.2 LULC Change Matrix (1989-2019)

LULC matrix (Table 2) reveals significant spatial transitions over time, particularly in conversion of barren land and vegetation into built-up areas, which aligns with the city's growing population and infrastructure demand (Jaganmohan et al., 2016).

From 2009 to 2019, 127.82 km² of barren land transitioned to built-up, and 6.49 km² converted into vegetation. A notable 243.33 km² of built-up areas remained unchanged. Water bodies exhibited minor transition, but their overall decline reflects increasing anthropogenic stress.

From 1999 to 2009, barren land continued transitioning into built-up (92.99 km²) and vegetation (27.20 km²), suggesting slight greening efforts. Vegetation loss to built-up (14.21 km²) and barren land (25.12 km²) underscores ecological stress during this urban expansion phase.

From 1989 to 1999, 65.41 km² of barren land transformed into built-up, and 20.62 km² of vegetation was also lost to construction. These transitions underline the early stages of urban-induced land use intensification.

Over the 30-year span (1989–2019), 173.04 km² of barren land and 57.13 km² of vegetation were transformed into built-up land, while only 23.96 km² of vegetation remained unchanged. This long-term shift highlights the irreversible nature of urban sprawl and its implications for ecological balance (Sajjad et al., 2015).

The observed LULC changes closely mirror Hyderabad's rapid urban growth, driven by sustained population expansion and infrastructural development. Between 1989 and 2019, Hyderabad's population increased significantly, reaching an estimated 10.8 million in 2023 (GHMC, 2023). This demographic surge, supported by municipal boundary extensions and economic diversification-particularly the growth of IT and industrial zones-has intensified land conversion pressures.

The LULC matrix (Table 3) illustrates substantial transformation of barren land (173.04 km²) and vegetation (57.13 km²) into built-up areas, especially after 2009, reflecting intensified urban infill and sprawl. The establishment of hubs like HITEC City and Gachibowli, alongside the merging of 51 villages and upcoming inclusion of 24 municipalities into GHMC, underscores the spatial footprint of this growth. These transitions not only signal the irreversible urban expansion of Hyderabad but also highlight the environmental stress caused by declining green cover and shrinking water bodies. Urban planning must now address this imbalance by integrating green infrastructure, compact growth strategies, and climate-resilient policies.

Table 3. LULC Change Matrix from 1989 to 2019

Year	2009-2019 (km²)	1999-2009 (km²)	1989-1999 (km²)	1989-2019 (km²)
Barren land	99.70	182.92	218.84	105.79
Barren land-Built-up	127.82	92.99	65.41	173.04
Barren land-Vegetation	6.49	27.20	7.73	12.55
Barren land-Waterbody	0.50	0.50	0.47	0.98
Built-up-Barren land	82.64	25.61	41.46	71.28
Built-up-Built-up	243.33	229.17	183.86	156.73
Built-up-Vegetation	9.87	15.14	18.03	15.41
Built-up-Waterbody	1.33	0.62	1.35	1.24
Vegetation-Barren land	43.90	25.12	42.56	48.65

Year	2009-2019 (km^2)	1999-2009 (km^2)	1989-1999 (km^2)	1989-2019 (km^2)
Vegetation-Built-up	15.82	14.21	20.62	57.13
Vegetation-Vegetation	36.07	51.48	65.46	23.96
Vegetation-Waterbody	1.42	1.14	2.95	1.82
Waterbody-Barren land	1.15	0.91	0.86	1.70
Waterbody-Built-up	0.80	0.84	0.65	0.88
Waterbody-Vegetation	2.28	3.41	0.74	2.79
Waterbody-Waterbody	9.52	11.48	11.86	8.75

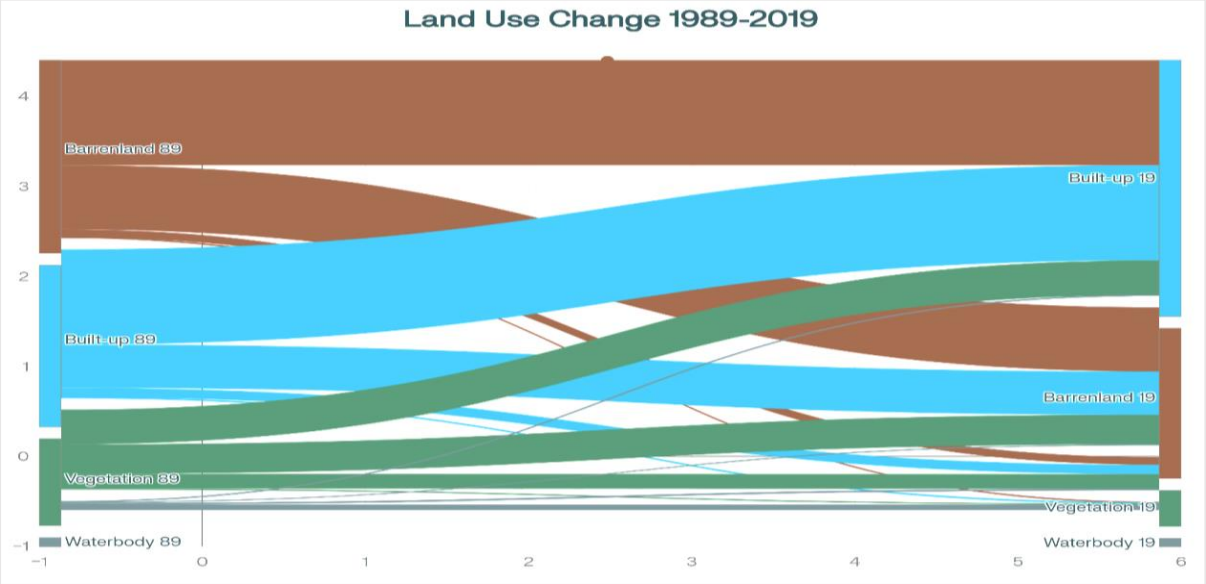

Figure 4. Sankey Diagram of LULC Transitions (1989–2019)

The transitions between 1989 and 2019 (Figure 4) reveal a clear narrative of urban expansion and land-cover persistence: the largest flow-173.04 km² of barren land becoming built-up highlights how previously marginal, undeveloped tracts have been targeted for infrastructure and residential growth, while another 57.13 km² of vegetated areas were cleared for construction, underscoring deforestation and loss of ecosystem services; concurrently, 156.73 km² of already built-up land remained urban, indicating core city footprints' stability even as edges expanded, and 105.79 km² of barren land and 23.96 km² of vegetation persisted unchanged, representing landscapes-such as deserts, rocky outcrops, protected forests, or parks-that either resist development or are maintained for conservation, together illustrating a dynamic interplay of growth at the margins and resilience at the core.

5.3 LST Variation in Hyderabad Over the Last 40 Years (in 10-year Intervals)

LST analysis indicates a clear warming trend across Hyderabad, with the mean surface temperature increasing from 29.9°C in 1989 to 31.67°C in 2019 (Table 4, Figure 5). The only deviation occurred in 2009, when mean LST dropped to 28.57°C, likely influenced by enhanced vegetation cover and anomalous climatic conditions during an unusually wet monsoon season that promoted evaporative cooling and reduced surface heating (IMD, 2009; Bala et al., 2021; Sai Bhargavi et al., 2021).

Between 1989 and 1999, both mean and maximum LST increased notably across vegetation and built-up areas, indicating a shift toward surfaces with higher heat retention. Water bodies, in contrast, showed relatively lower maximum LST, reinforcing their role as thermal moderators.

During 1999–2009, a temporary cooling phase was evident across most classes, particularly vegetation and water bodies, reflecting microclimatic improvements and favorable moisture conditions. Built-up zones also exhibited slightly reduced LST, possibly linked to slower construction activity and increased greenery.

From 2009 to 2019, LST values rose sharply across all LULC categories. The built-up areas recorded the highest mean (38.48°C) and maximum (43.72°C) temperatures, accentuating the urban heat island (UHI) effect (Weng et al., 2004). Barren land also exhibited elevated LST (mean 32.34°C), while vegetation and water bodies remained relatively cooler, though with diminishing cooling efficiency due to spatial contraction.

Table 4. LST Data of Hyderabad City Across LULC Classes

Land surface temperature																
	2019				2009				1999				1989			
	Min.	Max.	Mean	Std. dev.	Min.	Max.	Mean	Std. dev.	Min.	Max.	Mean	Std. dev.	Min.	Max.	Mean	Std. dev.
Waterbody	23.68	38.53	26.89	2.74	21.5	32.46	23.18	1.32	21.5	33.26	24.43	1.57	20.62	34.46	23.04	1.51
Vegetation	23.79	38.49	31.97	2.06	21.5	34.06	27.53	1.77	21.5	38	28.31	2.4	21.06	35.65	27.72	2.39
Barren land	24.24	40.25	32.34	1.5	23.25	35.65	29.65	1.54	22.82	36.83	31.75	1.72	23.25	35.65	31.26	1.21
Built-up	24.44	43.72	38.48	1.61	21.5	36.44	28.33	1.36	22.38	37.61	30.24	1.43	21.5	36.05	29.85	1.49

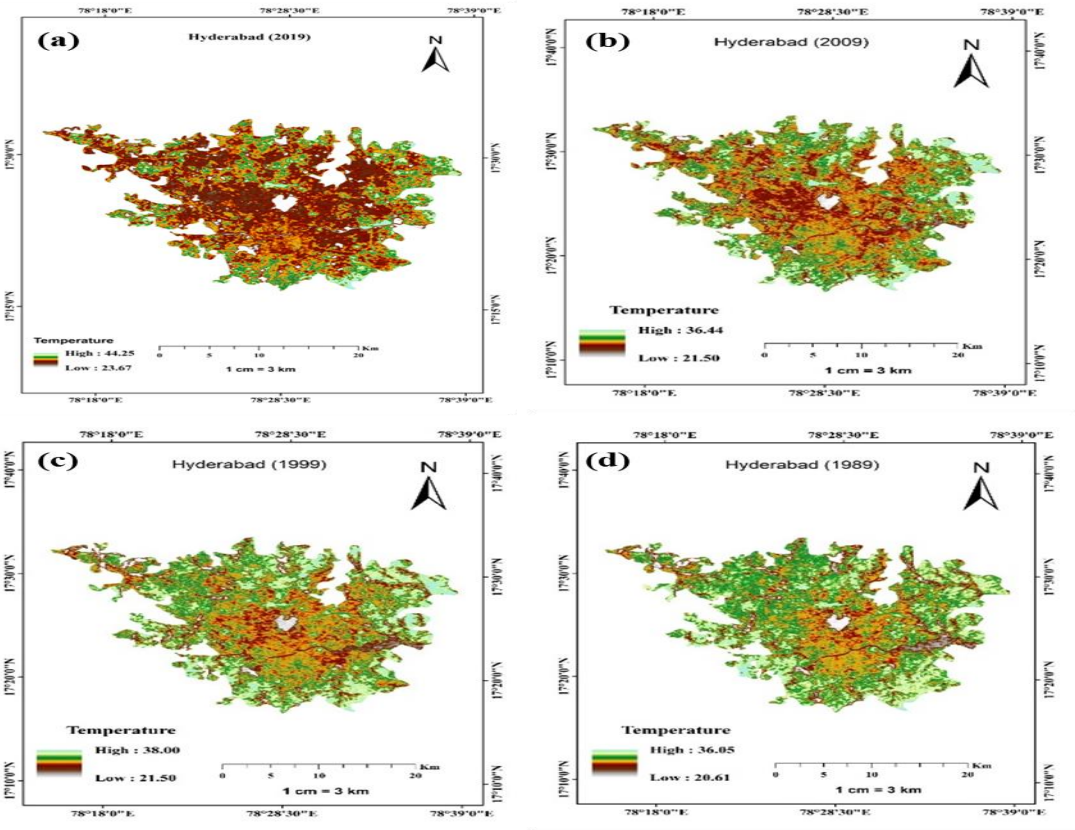

Figure 5. LST of Hyderabad Region for the Years (a) 2019, (b) 2009, (c) 1999, and (d) 1989

5.4 Spectral indices

5.4.1 NDBI

The NDBI values from 1989 to 2019 reveal an increasing spatial spread of urbanized land. However, the declining trend in mean NDBI suggests that while urban extent has increased, urban density has become more heterogeneous, possibly due to the emergence of peri-urban low-rise zones (Figure 6) (Yasin et al., 2022). This pattern also indicates sprawl-dominated growth rather than vertical compaction. Interestingly, despite the sharp increase in built-up land cover, the Normalized Difference Built-up Index (NDBI) exhibited a slight decline over time. This suggests that urban expansion in Hyderabad has predominantly taken the form of low-rise, horizontally spread development rather than compact, high-density growth. Additionally, the mixed spectral response in peri-urban areas-due to vegetation intermixing, reflective roofing, or semi-paved surfaces-may also contribute to lower NDBI values, highlighting the complexity of urban morphology in index-based classification."

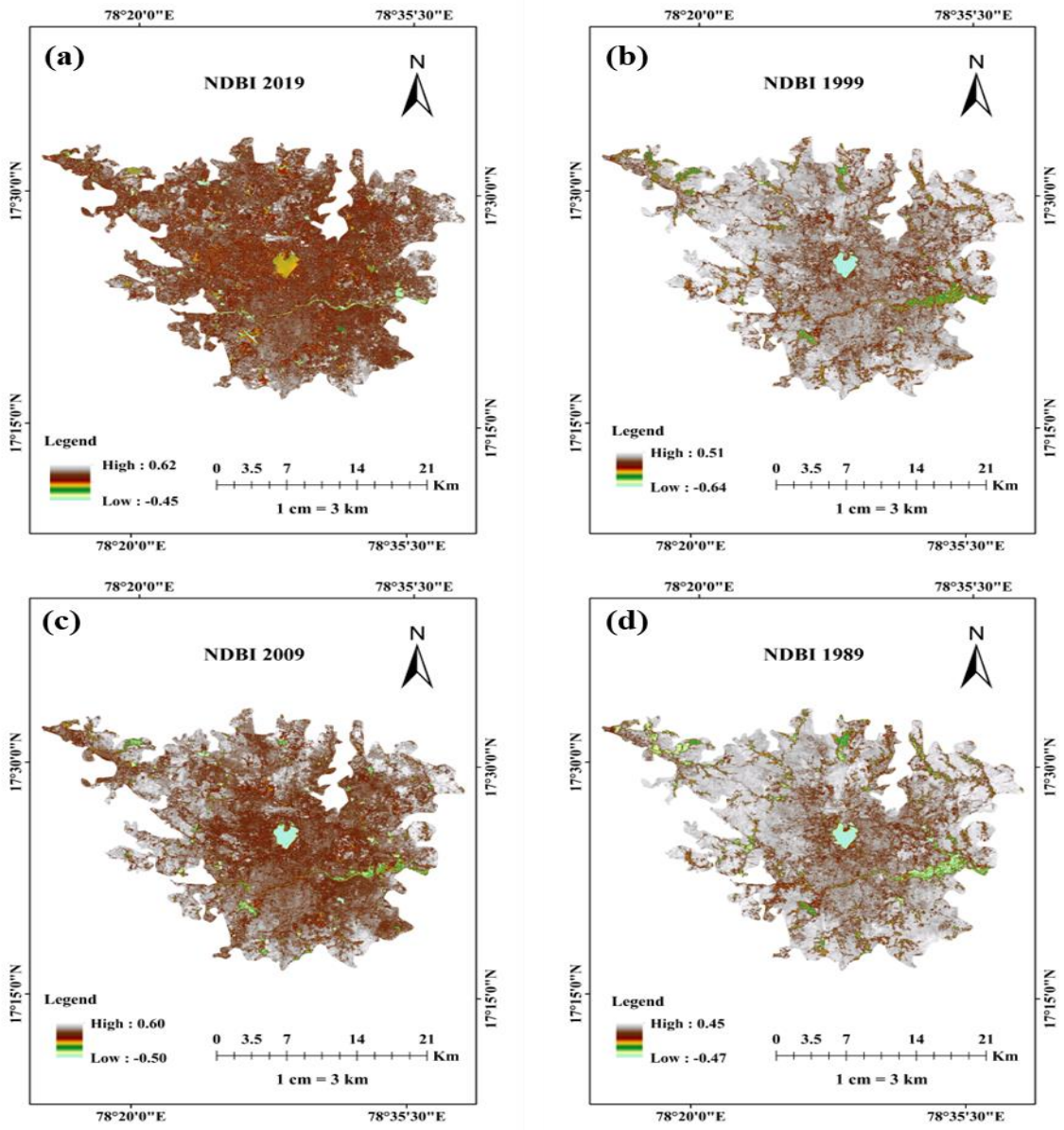

Figure 6. NDBI of Hyderabad Region for the Years (a) 2019, (b) 2009, (c) 1999 and (d) 1989

NDVI

NDVI trends demonstrate fluctuations: a rise between 1989 and 1999, a decline by 2009, and a modest increase again by 2019 (Figure 7). These fluctuations indicate alternating periods of vegetation growth and stress, likely linked to changing land management policies and climatic variations (Xu et al., 2016). The overall decline in mean NDVI from 1989 to 2019 indicates reduced vegetation health and density, aligning with trends of urban ecosystem degradation.

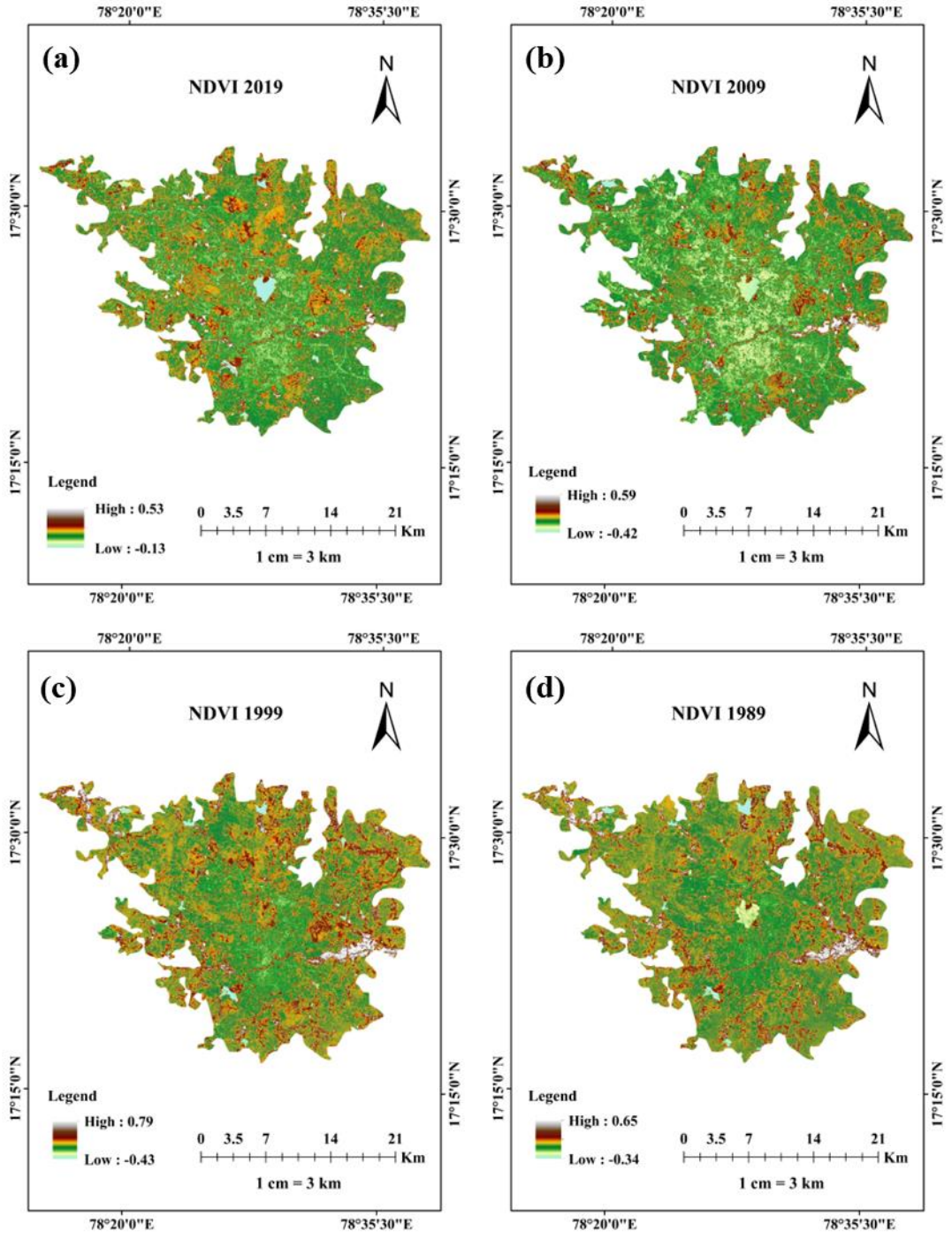

Figure 7. NDVI of Hyderabad Region for the Years (a) 2019, (b) 2009, (c) 1999 and (d) 1989

5.4.2 NDWI

NDWI values increased between 1989 and 1999, indicating improved water presence or quality, possibly due to reservoir management efforts (Figure 8). However, from 1999 to 2019, the decline in NDWI suggests a worsening water quality or shrinkage in water spread area, confirming observations from other Indian urban centers facing hydrological stress (Kafrawy et al., 2017).

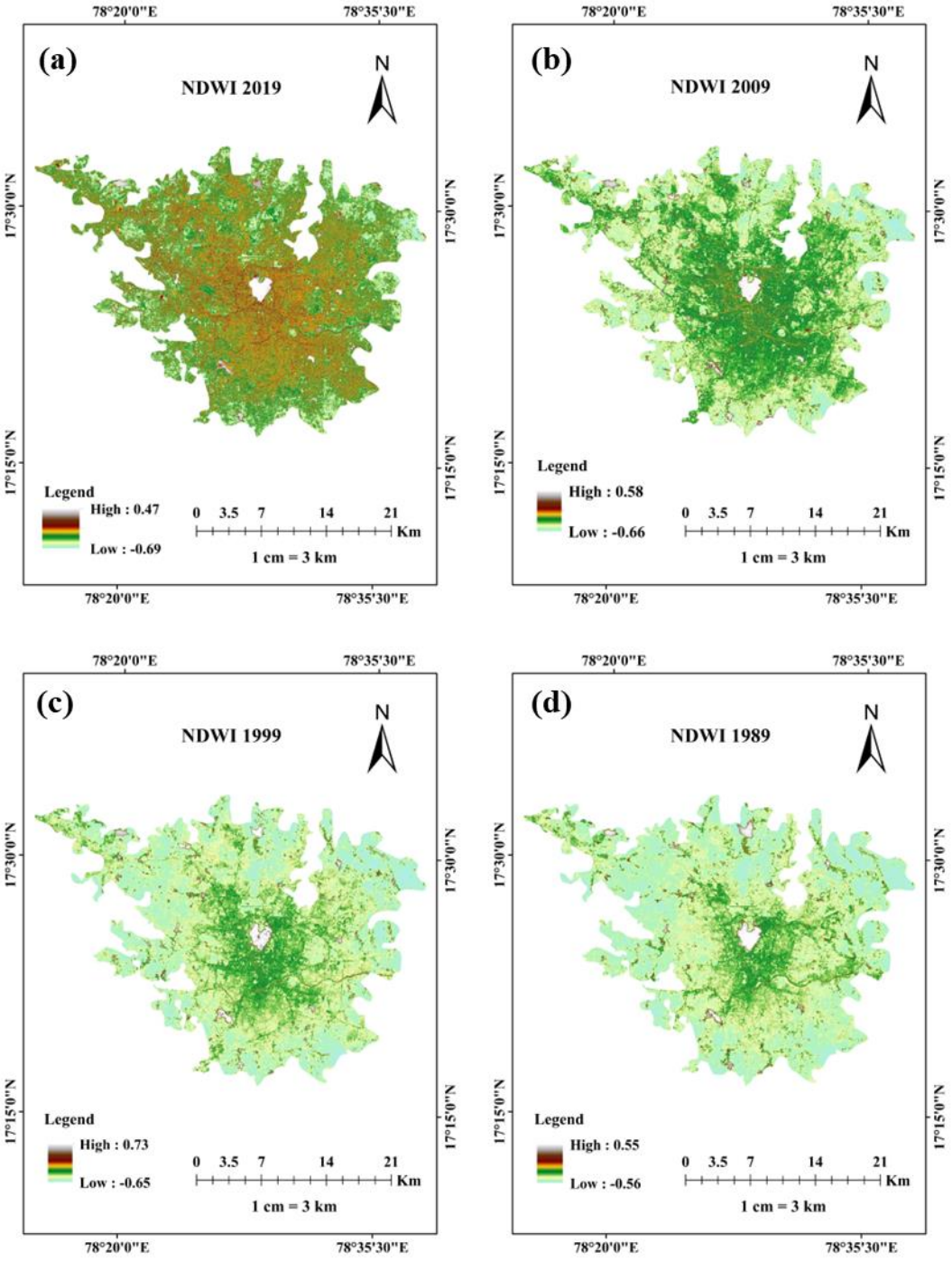

Figure 8. NDWI of Hyderabad Region for the Years (a) 2019, (b) 2009, (c) 1999 and (d) 1989

5.4.3 NDBaI

NDBaI values showed a decreasing trend from 1989 to 2019, indicating a transition from primary barren to cultivated or mixed-use barren land (Figure 9). This transformation suggests partial land utilization, possibly for informal agriculture or peri-urban development. The shift also supports the observed decline in barren land area in the LULC classification (Moisa et al., 2022; Zhao and Chen, 2005).

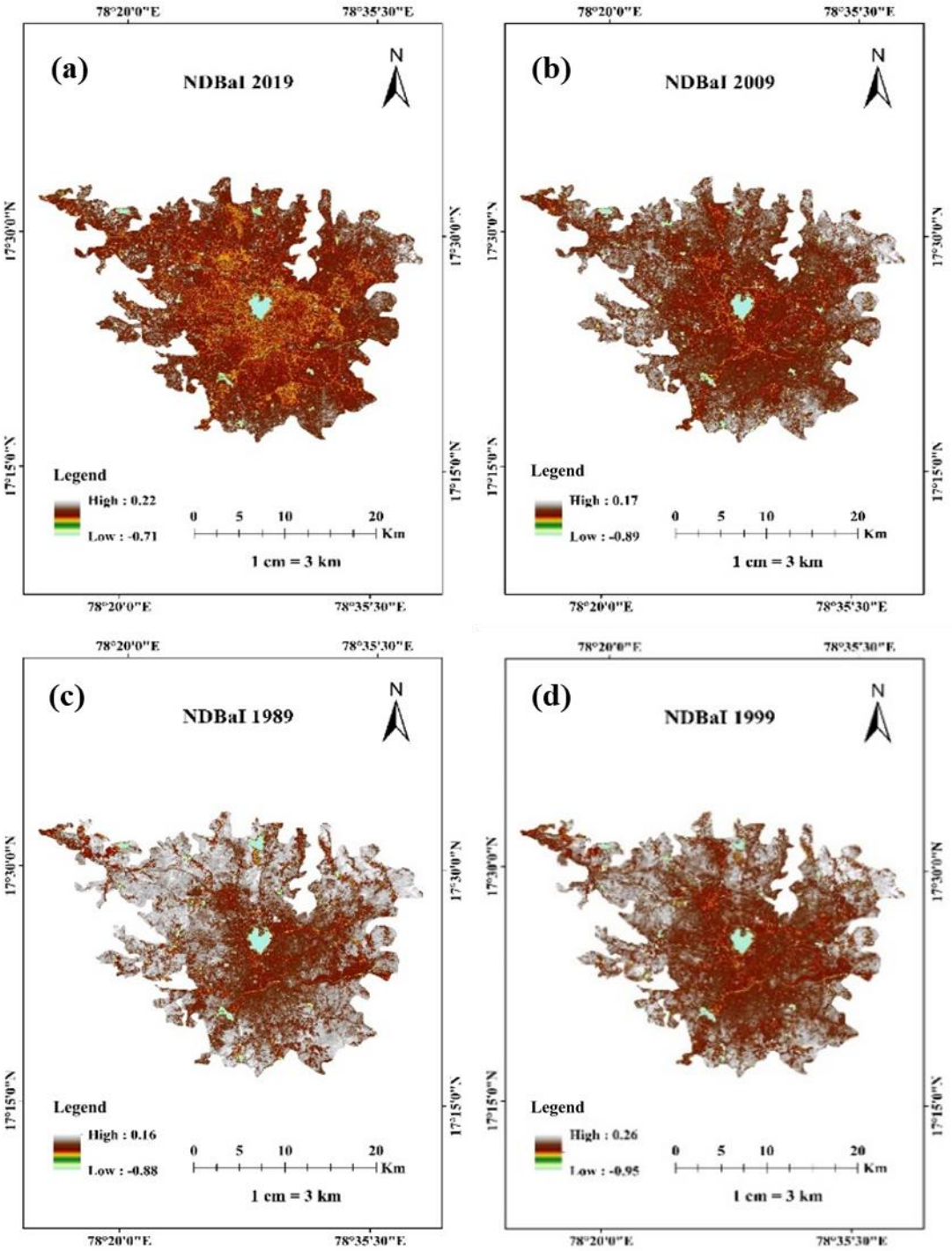

Figure 9. NDBaI of Hyderabad Region for the Years (a) 2019, (b) 2009, (c) 1999 and (d) 1989

5.5 Temporal Distribution of Remote Sensing Indices

The violin-plot analysis of NDVI, NDWI, NDBI, and NDBaI over four decades Hyderabad reveals a coherent narrative of land-cover transformation driven by urbanization (Figure 10). Vegetation vigor (NDVI) steadily weakened, as shown by progressively narrower, left-shifted distributions, mirroring loss of green cover to built-up and barren surfaces. Water indices (NDWI) also trended downward, signifying contraction of aquatic features and increased hydrological stress from impermeable expansion. Built-up intensity (NDBI) climbed sharply between 1989 and 2009-coinciding with the rise of IT corridors and industrial zones-but eased slightly by 2019, suggesting a move toward lower-density, horizontal growth in peri-urban fringes. In contrast, barren-area signature (NDBaI) declined throughout, reflecting the conversion of idle lands into either developed or vegetated areas. Collectively, these shifts capture how population pressures, infrastructural sprawl, and land-use policies have reshaped Hyderabad's surface characteristics over thirty years.

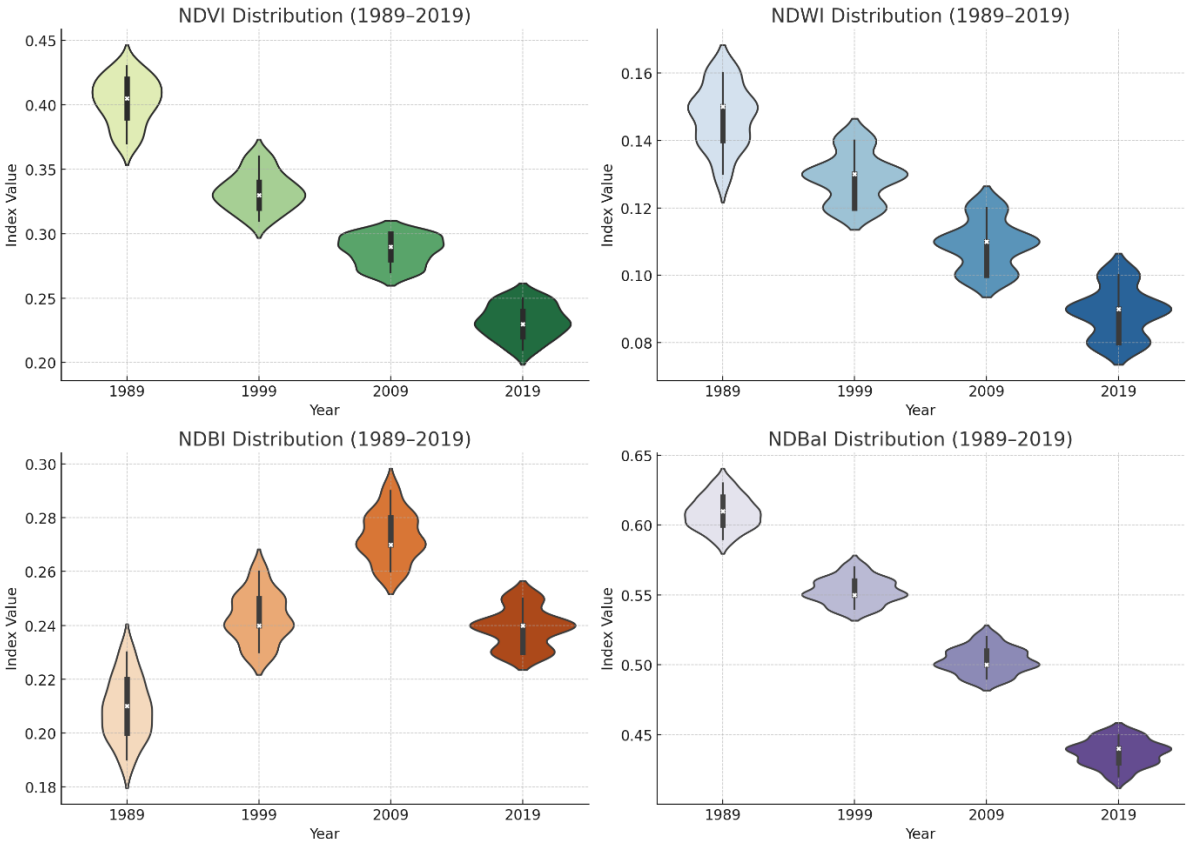

Figure 10. Violin plots showing the distribution of remote sensing indices (NDVI, NDWI, NDBI, and NDBaI) across the years 1989, 1999, 2009, and 2019 for Hyderabad city.

5.6 Correlation Analysis between LST and Spectral Indices (NDVI, NDWI, NDBI, NDBaI)

To quantify the relationships between land cover characteristics and thermal response, Pearson correlation coefficients were computed between LST and the following spectral indices: NDVI, NDWI, NDBI and NDBaI for each of the four study years (Table 5).

Table 5. Pearson Correlation Coefficients between LST and Spectral Indices

Year	LST–NDVI	LST–NDWI	LST–NDBI	LST–NDBaI
1989	-0.62	-0.45	+0.56	+0.49

1999	-0.58	-0.48	+0.63	+0.52
2009	-0.65	-0.43	+0.51	+0.46
2019	-0.68	-0.53	+0.67	+0.59

NDVI (Vegetation Index): A consistently strong negative correlation with LST (ranging from -0.58 to -0.68) indicates that vegetated areas exert a cooling effect on surface temperature, due to higher evapotranspiration and surface shading. The increasing strength of this relationship from 1989 to 2019 reflects the growing thermal impact of vegetation loss in the urban core.

NDWI (Water Index): The moderate negative correlation with LST suggests that water bodies and moisture-rich surfaces contribute to thermal regulation. However, the lower magnitude relative to NDVI reflects the declining spatial presence of open water within the urban landscape.

NDBI (Built-up Index): Strong positive correlations with LST (from +0.51 to +0.67) emphasize the thermal amplification caused by dense impervious surfaces such as concrete and asphalt. The 2019 peak indicates maximum built-up expansion and UHI intensification.

NDBaI (Barren Index): A moderate to strong positive correlation (up to +0.59 in 2019) reveals the heat-retaining characteristics of exposed soils and dry, unvegetated surfaces. Its rising trend suggests the role of transitional barren lands in contributing to LST elevation.

5.7 Gross urban density

The analysis of gross density values reveals a marked intensification in urban development across Hyderabad over the three-decade period. Gross density increased from approximately 1.19 in 1989 to 3.77 in 2019 (Table 6), indicating a significant rise in the compactness and intensity of built-up areas. This upward trend correlates strongly with the LULC transformation, wherein the built-up area expanded substantially from 35.8% in 1989 to 56.5% in 2019. This indicates that Hyderabad's urban land development became much more intensive. The growing urban density reflects urban infill, vertical expansion, or reducing open spaces within the urban area, rather than just horizontal sprawl (Shaban et al., 2020; Sridhar and Monkkonen, 2024).

Table 6. Gross Density Values over Years (1989–2019)

Year	1989	1999	2009	2019
Gross urban density	1.194	1.318	1.636	3.765

5.8 Contribution Index

CI quantifies the contribution of each LULC class to LST variation, reflecting their respective roles in surface heat mitigation or amplification (Table 7). Over the study period: Water bodies maintained consistently negative CI values (–0.14 to –0.11), reaffirming their cooling effect. However, the declining extent and deteriorating quality-indicated by decreasing NDWI-have reduced their overall cooling efficiency. Vegetation also exhibited a cooling influence, but its CI decreased markedly (from –0.42 to –0.07), mirroring the NDVI decline and the loss of green cover due to rapid urban expansion. Barren land showed the strongest initial heating effect (0.58 in 1989), which declined steadily to 0.24 by 2019, likely reflecting its transformation into cultivated or semi-permeable surfaces. Built-up areas occasionally recorded slightly negative CI values (–0.02 to –0.12), possibly linked to reflective roofing, urban greenery, or low-rise morphology. Nonetheless, they remain significant contributors to surface heating through anthropogenic emissions and heat retention.

Table 7. CI of LULC Classes in the City

Class / Year	1989	1999	2009	2019
CI (Water)	-0.14	-0.15	-0.11	-0.11
CI (Vegetation)	-0.42	-0.3	-0.15	-0.07
CI (Barren Land)	0.58	0.55	0.37	0.24
CI (Built-up)	-0.02	-0.11	-0.12	-0.05

6. Discussion

The observed LULC dynamics in Hyderabad over the three-decade span reflect an accelerated urban transformation, with profound implications for LST regulation, ecological balance, and spatial thermal inequities. While the result section quantified LULC transitions and LST variations, the present discussion aims to interpret these patterns in a broader environmental, climatological, and urban planning context.

6.1 Urban Expansion and Landscape Reconfiguration

The significant reduction in vegetation and barren land in favor of built-up expansion demonstrates the city's shifting landscape trajectory, largely influenced by post-liberalization economic growth, IT sector proliferation, and infrastructure-led development. Comparable trends have been reported across Indian metropolises such as Bengaluru and Pune, where land cover conversions have not only altered surface compositions but disrupted ecosystem services (Jaganmohan et al., 2016; Das and Das, 2020). Notably, the fragmentation and assimilation of open land into impervious urban forms suggest a pattern of unregulated sprawl, which undermines green-blue networks critical for microclimatic balance.

6.2 Thermal Impacts and Urban Heat Intensification

The increasing LST align with a growing urban heat island (UHI) signature, substantiating the thermally amplified effect of impervious surfaces, as established in urban climatology literature (Weng et al., 2004; Saranya et al., 2022). The built-up areas, while varying in spatial density as reflected in declining NDBI values, consistently exhibit thermal dominance-confirming that structural composition (e.g., concrete, asphalt), rather than density alone, governs urban heat contribution.

Moreover, the apparent decrease in LST in 2009, in contrast to the overall warming trend, likely signifies a localized climatic anomaly or temporary vegetation recovery. Such fluctuations underscore the influence of inter-annual climate variability, monsoonal performance, or conservation interventions, warranting integration of meteorological datasets in future LST analyses.

6.3 Role of Vegetation and Water in Thermal Regulation

The diminishing thermal mitigation capacity of vegetation and water bodies, as indicated by declining CI values, is a critical concern. Vegetation's reduced capacity to cool the urban environment can be traced not only to spatial loss but also to physiological stress, as NDVI values suggest declining health and coverage (Xu et al., 2016). Similarly, decreasing NDWI values signal compromised waterbody function, likely due to eutrophication, encroachment, or hydrological fragmentation-concerns raised in comparable urban studies from Ahmedabad and Chennai (Kafrawy et al., 2017; Nagarajan et al., 2020).

These insights affirm that mere presence of natural features does not guarantee ecological service delivery; their quality, connectivity, and protection are equally vital for sustaining urban resilience.

6.4 Barren Land Conversion and Changing Heat Contribution

Interestingly, barren land, traditionally perceived as a heat-amplifying surface, shows a decreasing CI contribution over time. This trend likely reflects its conversion into cultivated or semi-permeable zones, as also indicated by declining NDBaI values (Moisa et al., 2022). While this suggests partial ecological recovery, it does not equate to ecosystem restoration, given the potential absence of vegetation structure or diversity. The thermal profile of modified barren land remains subject to surface albedo, moisture retention, and material type-factors not directly captured by basic LULC categories but vital for urban climate governance.

6.5 Interpretation of Spectral Indices as Diagnostic Tools

The application of NDVI, NDWI, NDBI, and NDBaI indices enhances diagnostic capacity for understanding the thermal and ecological dynamics of Hyderabad's urbanization. For instance, declining NDVI alongside increasing LST highlights vegetation stress, while decreasing NDWI alongside increasing LST in water-proximal zones suggests a weakening of aquatic buffers. These interpretations are consistent with index-based urban thermal assessments in Cairo and Shanghai (Kafrawy et al., 2017; Zhao and Chen, 2005).

Notably, the observed decline in NDBI despite built-up area expansion may be attributed to dispersed, low-density sprawl or increased rooftop vegetation, although these possibilities require further ground validation. This finding cautions against over-reliance on spatial coverage alone as an indicator of urban thermal stress and calls for integrating material composition, shading, and reflectivity into UHI models.

6.6 Urban Sustainability and Adaptive Strategies

The thermal implications of Hyderabad's urban evolution reinforce the urgency for sustainable land-use planning. Strategic measures-such as green infrastructure development, riparian corridor restoration, and promotion of high-albedo materials-are imperative to counteract rising LSTs. Additionally, land-use zoning should prioritize vegetated buffers around urban cores, as supported by CI trends demonstrating the diminishing role of natural covers in thermal moderation.

From a governance perspective, the study underscores the need for integrated spatial planning that harmonizes urban growth with climate adaptation. Decision-makers can leverage CI-based zoning to target intervention zones where land covers either intensify or mitigate urban warming. Moreover, the synergistic use of SVM classification and multi-index analysis, as demonstrated in this study, offers a replicable framework for monitoring urban climate-health linkages across Indian cities.

6.7 Outlook and Research Directions

While this study effectively captures decadal LULC and LST trends, its temporal resolution is limited by four snapshot years. Incorporating seasonal or monthly datasets from Sentinel or MODIS platforms would enhance temporal granularity. Furthermore, integrating socio-economic, energy use, and pollution datasets would facilitate a multi-scalar understanding of UHI dynamics and inform policy across urban-rural gradients.

Additionally, future research should explore feedback loops between land cover change and ecosystem disservices (e.g., reduced evapotranspiration, surface runoff), and examine equity implications of UHI exposure among different socio-economic groups-a growing concern in climate-justice discourse (Yengoh et al., 2017; Sai Bhargavi et al., 2021).

7. Conclusion

This study provides a comprehensive assessment of LULC changes and their influence on LST across Hyderabad from 1989 to 2019. The built-up area has expanded significantly-from 35.81% to 56.49%-at the expense of vegetated areas, water bodies, and barren lands. The reduction in vegetation (from 19.39% to 8.20%) and the concurrent stress reflected through NDVI values indicate increased ecological vulnerability, while the declining

NDWI and NDBaI values point to worsening water quality and transformation of primary barren land into cultivated forms.

The CI effectively captured the role of various land cover classes in modulating LST. While barren land consistently contributed to increased surface temperatures, water bodies and vegetated areas served as thermal buffers-though with declining efficiency over time. Notably, built-up areas displayed a marginal and fluctuating thermal role, underscoring the complexity of urban heat interactions influenced by density, material composition, and land morphology.

These findings underscore the crucial role of multi-temporal satellite datasets in deciphering long-term urban environmental dynamics. The integration of indices such as NDVI, NDWI, NDBI, and NDBaI enhances our capacity to understand surface transformations beyond simple classification, offering nuanced insights into the state of urban ecosystems.

The study further highlights the pressing need for data-driven urban planning that integrates green infrastructure, hydrological restoration, and microclimate-sensitive design to mitigate UHI effects and enhance thermal comfort. As urban green areas diminish under demographic pressure, their strategic conservation becomes imperative for sustaining urban livability. Moreover, the interplay of latent heat flux and cloud cover contributes to urban thermal variations, particularly evident in elevated nighttime temperatures and moderated daytime heat.

However, the current analysis is limited by the absence of atmospheric and structural variables such as wind flow, pollution load, and vertical urban morphology. To strengthen future assessments, we recommend integrating datasets on population dynamics, climate-resilient city indices, and nature-based solutions. Forecasting models using fine-resolution temporal imagery can offer predictive insights essential for proactive environmental governance.

Competing Interest declaration: Authors have no conflict of interest to declare.

Funding: The authors did not receive support from any organization for the submitted work.

Availability of data and material: Not applicable.

Ethics, Consent to Participate, and Consent to Publish declarations: Not applicable.

Clinical trial registration: This study is not a clinical trial.

Author contributions: Pardeep Kumar: Original Idea, Conceptualization, Data Analysis, Paper Writing, Paper Review. Pratyush Verma: Data Collection, Conceptualization, Paper Writing. Saumitra Mukherjee: Conceptualization, Paper Review. Bir Abhimanyu Kumar: Paper Review, Bhawna Yadav: Paper writing.

References

[1] Abdulmana, S., Lim, A., Wongsai, S., and Wongsai, N. (2021). Land surface temperature and vegetation cover changes and their relationships in Taiwan from 2000 to 2020. Remote Sensing Applications: Society and Environment, 24, 100636.
[2] Akbari, H. (2009). Cooling our communities. A guidebook on tree planting and light-colored surfacing.
[3] Arnfield, A. J. (2003). Two decades of urban climate research: a review of turbulence, exchanges of energy and water, and the urban heat island. International Journal of climatology, 23(1), 1-26.
[4] Bahl, H. D., and Padmanabhamurty, B. (1979). Heat island studies at Delhi. Mausam, 30(1), 119-122.
[5] Bala, R., Prasad, R., & Yadav, V. P. (2021). Quantification of urban heat intensity with land use/land cover changes using Landsat satellite data over urban landscapes. Theoretical and Applied Climatology, 145, 1–12. https://doi.org/10.1007/s00704-021-03610-3.
[6] Bokaiea, M., M. K. Zarkesha, P. D. Arastehb, and H. Ali. (2016). “Assessment of Urban Heat Island Based on the Relationship between Land Surface Temperature and Land Use/Land Cover in Tehran.” Sustainable Cities and Society 23: 94–104. doi: 10.1016/j.scs.2016.03.009.
[7] Bridgman H., Warner R. and Dodson J., (1995) "Urban Biophysical Environments". Oxford University Press, Melbourne, p. 152, 1995.

[8] Bunai, T., Rokhmatuloh, A. W., Wibowo, A., and Shidiq, I. P. A. (2017). Comparison spatial pattern of land surface temperature with mono window algorithm and split window algorithm: a case study in south Tangerang, Indonesia. Series: Earth and Environmental Science, 149.

[9] Chatterjee, S., Khan, A., Dinda, A., Mithun, S., Khatun, R., Akbari, H., and Wang, Y. (2019). Simulating micro-scale thermal interactions in different building environments for mitigating urban heat islands. Science of the Total Environment, 663, 610-631.

[10] Chen, F., Yang, X., and Gallo et al. 1999 Zhu, W. (2014). WRF simulations of urban heat island under hot-weather synoptic conditions: The case study of Hangzhou City, China. Atmospheric Research, 138, 364-377.

[11] Chen, X. L., H. M. Zhao, P. X. Li, and Z. Y. Yin. (2006). "Remote Sensing Image-Based Analysis of the Relationship between Urban Heat Island and Land Use/Cover Changes." Remote Sensing of Environment 104: 133–146. doi: 10.1016/j.rse.2005.11.016.

[12] Cui L., Shi J., 2012. Urbanization and its environmental effects in Shanghai, China. Urban Climate 2: 1–15. DOI 10.1016/j.uclim.2012.10.008.

[13] Doan, Q. V., and Kusaka, H. (2015). Numerical study on regional climate change due to the rapid urbanization of greater Ho Chi Minh City's metropolitan area over the past 20 years. International Journal of Climatology, 36(10), 3633-3650.

[14] Eludoyin, O. M., I. O. Adelekan, R. Webster, and A. O. Eludoyin. (2013). "Air Temperature, Relative Humidity, Climate Regionalization and Thermal Comfort of Nigeria." International Journal of Climatology. http://onlinelibrary.wiley.com/doi/10.1002/joc.3817.

[15] Estoque, R. C., Y. Murayama, and S. W. Myint. (2017). "Effects of Landscape Composition and Pattern on Land Surface Temperature: An Urban Heat Island Study in the Megacities of Southeast Asia." Science of the Total Environment 577: 349–359. doi: 10.1016/j.scitotenv.2016.10.195.

[16] Gallo, K. P., T. W. Owen, D. R. Easterling, and P. F. Jamason. (1999). "Temperature Trends of the U.S. Historical Climatology Network Based on Satellite-Designated Land Use/Land Cover." Journal of Climate 12: 1344–1348. doi:10.1175/1520-0442(1999)0122.0.CO;2.

[17] Gangadharan, V. K., Sasidharan, N. V., and Santhosh, K. (1999). A STUDY ON HEAT ISLAND INTENSITIES AT THIRUVANTHAPURAM ON A COLD WINTER NIGHT. Mausam, 50(1), 106-108.

[18] Gemeda, D. O., Kenea, G., Teshome, B., Daba, G. L., Argu, W., and Roba, Z. R. (2024). Impact of land use and land cover change on land surface temperature: Comparative studies in four cities in southwestern Ethiopia. Environmental Challenges, 16, 101002.

[19] Gogoi, P. P., and Vinoj, V. (2025). Land Use Land Cover as a Potential Driver of Surface Air Temperature Change Over India. Meteorological Applications, 32(3), e70061.

[20] Guha, S., and Govil, H. (2025). Evaluating the stability of the relationship between land surface temperature and land use/land cover indices: a case study in Hyderabad city, India. Geology, Ecology, and Landscapes, 9(1), 231-243.

[21] Hahs A.K., McDonnell M.J., McCarthy M.A., Vesk P.A., Corlett R.T., Norton B.A., Clemants S.E., Duncan R.P., Thompson K., Schwartz M.W., Williams N.S.G., (2009). A global synthesis of plant extinction rates in urban areas. Ecology Letters 12: 1165–1173. DOI 10.1111/j.1461- 0248.2009.01372.x.

[22] Hamdi, R. and G. Schayes, (2008). "Sensitivity Study of the Urban Heat Island Intensity to Urbancharacteristics." International Journal of Climatology 28: 973–982. doi:10.1002/(ISSN) 1097-0088.

[23] Helmers D.P. (2010). Housing growth in and near United States protected areas limits their conservation value. Proceedings of the National Academy of Sciences 107(2): 940–945. DOI 10.1073/pnas.0911131107.

[24] Howard, L. (2012). The climate of London: deduced from meteorological observations (Vol. 1). Cambridge University Press.

[25] INDIA, P. (2011). Census of India 2011 provisional population totals. New Delhi: Office of the Registrar General and Census Commissioner.

[26] Jago-on K.A.B., Kaneko S., Fujukura R., Fujiwara A., Imai T., Matsumoto T., 2009. Urbanization and subsurface environmental issues: An attempt at DPSIR model application in Asian cities. Science of the total Environment 407(9): 3089–3104. DOI 10.1016/j.scitotenv.2008.08.004.

[27] Kafrawy, S. B. E., Donia, N. S., and Mohamed, A. M. (2017). Water quality assessment based on CWQI and NDWI indices in Mariout Lake, Egypt. MOJ Ecology Environmental Sciences, 2(5), 00039.
[28] Kawashima, S. (1994). "Relation between Vegetation, Surface Temperature and Surface Composition in the Tokyo Region during winter." Remote Sensing of Environment 50: 52–60. doi:10.1016/ 0034-4257(94)90094-9.
[29] Khan, M. A., and Syed, N. A. (2015). Image processing techniques for automatic detection of tumor in human brain using SVM. Int J Adv Res Comput Commun Eng, 4(4).
[30] Kim Y.H., Baik J.J., (2005). Spatial and temporal structure of urban heat island in Seoul. Journal of Applied Meteorology 44: 591–605. DOI 10.1175/JAM2226.1.
[31] Landsat Project Science Office. (2002)." Landsat 7 Science Data User's Handbook." Goddard Space Flight Center, NASA, Washington, DC. https://landsat.gsfc.nasa.gov/wp-content/uploads/2016/ 08/Landsat7_Handbook.pdf.
[32] Liu J.G., Diamond J. (2005). China's environment in a globalizing world. Nature 435: 1179–1186. DOI 10.1038/4351179a.
[33] Moisa, M. B., Dejene, I. N., and Gemeda, D. O. (2022). Geospatial technology–based analysis of land use land cover dynamics and its effects on land surface temperature in Guder River sub-basin, Abay Basin, Ethiopia. Applied Geomatics, 14(3), 451-463.
[34] Ohwo O., Abotutu A., (2015). Environmental Impact of Urbanisation in Nigeria. British Journal of Applied Science and Technology 9(3): 212–221. DOI 10.9734/bjast/2015/18148.
[35] Oke T.R (1987). "Boundary Layer Climates". London. Methuen, pp.33-76.
[36] Oke T.R, (1995). "The heat island of the urban boundary layer: characteristics, causes and effects". In J.E. Cermak et al (eds.). Wind climate in cities, pp.81-107.
[37] Oke, T. R. (1982). The energetic basis of the urban heat island. Quarterly journal of the royal meteorological society, 108(455), 1-24.
[38] Oke, T. R., and Cleugh, H. A., (1987). Urban heat storage derived as energy balance residuals. Boundary-Layer Meteorology, 39(3), 233-245.
[39] Omran, E. E. (2012). "Detection of Land-Use and Surface Temperature Change at Different Resolutions." Journal of Geographic Information System 4: 189–203. doi:10.4236/jgis.2012.43024.
[40] Parker, D. E. (2010). Urban heat island effects on estimates of observed climate change. Wiley Interdisciplinary Reviews: Climate Change, 1(1), 123-133.
[41] Qiao, Z., G. Tian, and L. Xiao. (2013). "Diurnal and Seasonal Impacts of Urbanization on Theurban Thermal Environment: A Case Study of Beijing Using MODIS Data." ISPRS Journal of Photogrammetry and Remote Sensing 85: 93–101. doi: 10.1016/j.isprsjprs.2013.08.010.
[42] Radeloff V.C., Stewart S.I., Hawbaker T.J., Gimmi U., Pidgeon A.M., Flather C.H., Hammer R.B., Ramachandraia, C. (2013). Drinking water: issues in access and equity. PDF). Jointactionforwater.org. Archived from the original (PDF) on, 10 November 2013. Retrieved 18 November 2012.
[43] Rao, P. K. (1972). "Remote Sensing of Urban "Heat Islands" from an Environmentalsatellite." Bulletin of the American Meteorological Society 53: 647−648.
[44] Rees, G., Hebryn-Baidy, L., and Belenok, V. (2024). Temporal variations in land surface temperature within an urban ecosystem: A comprehensive assessment of land use and land cover change in Kharkiv, Ukraine. Remote Sensing, 16(9), 1637.
[45] Sabiha Sultana and A.N.V. Satyanarayana (2018): Urban heat island intensity during winter over metropolitan cities of India using remote-sensing techniques: impact of urbanization, International Journal of Remote Sensi.ng, DOI: 10.1080/01431161.2018.1466072.
[46] Saito I., Ishihara O. and Katayama T. (1990). "Study of the effect of green areas on the thermal environment in an urban area", Energy and Buildings, Vol. 15-16, pp.443-446.
[47] Schell L.M., Smith M.T. and Billsborough A., "Human biological approaches to the study of third world urbanism" (1993). In Schell.L.M. Smith M.T. and Billsborough A. (eds.). Urban ecology and health in the 3rd world, Cambridge University Press, pp. 1-9.

[48] Seto K.C., Fragkias M., Guneralp B., Reilly M.K. (2011). A meta-analysis of global urban land expansion. PLoS one 6(8): 1–9. DOI 10.1371/journal.pone.0023777.
[49] Shaban, A., Kourtit, K., & Nijkamp, P. (2020). India's urban system: sustainability and imbalanced growth of cities. Sustainability, 12(7), 2941.
[50] Sobrino, J. A., R. Oltra-Carrió, G. Sòria, R. Bianchi, and M. Paganini. (2012). "Impact of Spatial Resolution and Satellite Overpass Time on Evaluation of the Surface Urban Heat Island Effects." Remote Sensing of Environment 117: 50–56. doi: 10.1016/j.rse.2011.04.042.
[51] Sridhar, K. S., & Monkkonen, P. (2024). Urban form in India 1975–2015: Have India's cities become flat?. Cities, 145, 104705.
[52] Tian, B., Wang, L., Kashiwaya, K., and Koike, K. (2015). Combination of well-logging temperature and thermal remote sensing for characterization of geothermal resources in Hokkaido, northern Japan. Remote Sensing, 7(3), 2647-2667.
[53] Touchaei, A. G., and Wang, Y., (2015). Characterizing urban heat island in Montreal (Canada)-effect of urban morphology. Sustainable Cities and Society, 19, 395-402.
[54] Vancutsem, C., P. Ceccato, T. Dinku, and S. J. Connor. (2010). "Evaluation of MODIS Land Surface Temperature Data to Estimate Air Temperature in Different Ecosystems over Africa." Remote Sensing of Environment 114: 449–465. doi: 10.1016/j.rse.2009.10.002.
[55] Wang, F., Qin, Z., Song, C., Tu, L., Karnieli, A., and Zhao, S. (2015). An improved mono-window algorithm for land surface temperature retrieval from Landsat 8 thermal infrared sensor data. Remote sensing, 7(4), 4268-4289.
[56] Weng, Q. (2009). "Thermal Infrared Remote Sensing for Urban Climate and Environmental Studies: Methods, Applications, and Trends (Review Article)." ISPRS Journal of Photogrammetry and Remote Sensing 64: 335–344. doi: 10.1016/j.isprsjprs.2009.03.007.
[57] Xu, Y., Yang, J., and Chen, Y. (2016). NDVI-based vegetation responses to climate change in an arid area of China. Theoretical and Applied Climatology, 126, 213-222.
[58] Yasin, M. Y., Abdullah, J., Noor, N. M., Yusoff, M. M., and Noor, N. M. (2022, October). Landsat observation of urban growth and land use change using NDVI and NDBI analysis. In IOP Conference Series: Earth and Environmental Science (Vol. 1067, No. 1, p. 012037). IOP Publishing.
[59] Zhao S.Q., Da L.J., Tang Z.Y., Fang H.J., Song K., Fang J.Y. (2006). Ecological consequences of rapid urban expansion: Shanghai, China. Frontier Ecology and Environment 4(7): 341– 346. DOI 10.1890/1540-9295(2006)004[0341: ECORUE] 2.0. CO; 2.
[60] Zhao, H., and Chen, X. (2005, July). Use of normalized difference bareness index in quickly mapping bare areas from TM/ETM+. In International geoscience and remote sensing symposium (Vol. 3, p. 1666).
[61] Zhao, Q., Haseeb, M., Wang, X., Zheng, X., Tahir, Z., Ghafoor, S., ... and Almutairi, K. F. (2024). Evaluation of land use land cover changes in response to land surface temperature with satellite indices and remote sensing data. Rangeland Ecology and Management, 96, 183-196.
[62] Rozenstein, O., Qin, Z., Derimian, Y., & Karnieli, A. (2014). Derivation of land surface temperature for Landsat-8 TIRS using a split window algorithm. Sensors, 14(4), 5768-5780.
[63] Sai Bhargavi, T., & Singh Umesh, K. (2021). Synergic relation between urban pollution island and meteorological parameters over urban heat island for the city of Hyderabad during lockdown. Disaster Advances, 14 (8).